Zeitschrift: Helvetica Physica Acta
Band: 49 (1976)
Heft: 4

Artikel: Gamma-gamma angular correlation experiments using gaseous sources of 125Xe, 127Xe and 129mXe

Autor: Ledebur, Th.v.

DOI: https://doi.org/10.5169/seals-114788

Helvetica Physica Acta, Vol. 49 (1976), Birkhäuser Verlag, Basel

Gamma–Gamma Angular Correlation Experiments using Gaseous Sources of ^{125}Xe, ^{127}Xe and ^{129m}Xe[1])

by **Th. v. Ledebur**

Laboratory for High Energy Physics, Swiss Federal Institute of Technology, Zurich, Switzerland

(5. III. 1976)

Abstract. Employing gaseous sources of ^{125}Xe, ^{127}Xe and ^{129m}Xe gamma–gamma angular correlation experiments were performed. At low source pressures the resonance behavior of angular correlations in ^{125}I and ^{127}I in a weak external magnetic field were studied, and the resonance widths were found to be comparable with the natural widths. The possibility of determining short nuclear lifetimes from resonance measurements is discussed. The unperturbed angular correlation of cascades in ^{125}I, ^{127}I and ^{129}Xe was measured and the following correlation coefficients were determined: A_2(55–188 keV, ^{125}I) = 0.229 ± 0.008, A_2(172–203 keV, ^{127}I) = 0.2170 ± 0.0028, A_2(172–145 keV, ^{127}I) = −0.052 ± 0.011, A_2(145–58 keV, ^{127}I) = −0.2234 ± 0.0067, and A_2(196–40 keV, ^{129}Xe) = −0.159 ± 0.007. The mixing ratios deduced from these results are discussed. The magnetic moments of the $3/2^+$ states in ^{125}I, ^{127}I and ^{129}Xe were measured and found to be $\mu(3/2^+, {}^{125}\text{I}) = 2.2 \pm 0.7$ nm, $\mu(3/2^+, {}^{127}\text{I}) = 1.05 \pm 0.17$ nm and $\mu(3/2^+, {}^{129}\text{Xe}) = 0.74 \pm 0.20$ nm. The results are discussed with respect to the quasiparticle model.

1. Introduction

For a considerable time gaseous sources have seldom been used in angular correlation experiments. Leisi [1, 2] performed measurements at low source pressures and showed the existence of a resonance of the angular correlation in a weak external magnetic field. More recently, Gygax [3, 4] measured the angular correlation for different source pressures covering a large pressure range and observed an increase of the correlation with rising pressure.

The features which render gaseous sources attractive for the present experiments are the following:

For very low pressures the atoms may be considered isolated. Therefore, the only possible perturbation of the angular correlation is induced by the hyperfine interaction of the free atom. If the spin of the electronic shell is zero, this interaction vanishes and the angular correlation is necessarily unperturbed. On the other hand, a strong ionization of the atom (as occurs after an electron capture and subsequent Auger emissions) provides a very strong hyperfine interaction which gives rise to a resonance in a weak external magnetic field. Since the width of the resonance depends, except for atomic splitting factors, only on the lifetime of the intermediate nuclear level, resonance experiments may offer a method for measuring short nuclear lifetimes.

---

[1]) Thesis 5476, ETHZ 1975.

For sufficiently high source pressures the measurements of Gygax indicate that the angular correlation approximates to its unperturbed value, even if a preceding electron capture has caused a high degree of ionization in the atom. This can be explained by a random fluctuation of the direction of the electronic spin. If the frequency of the spin reorientation, which originates from the atomic collisions in the gas, is sufficiently high, the average electromagnetic fields at the nucleus vanish and the correlation is unperturbed. We shall show that unperturbed angular correlations and magnetic moments of excited nuclear states can be measured in these systems.

In Section 2 measurements of unperturbed correlations of cascades in ^{125}I and ^{127}I, using high-density gaseous sources, and of the 196–40 keV cascade in ^{129}Xe, using low-density sources, are described. Section 3 contains measurements of the resonance behavior of the perturbed angular correlation in low-density gaseous sources of ^{125}Xe and ^{127}Xe. In section 4 measurements of the magnetic moments of the $3/2^+$ states in ^{125}I, ^{127}I and ^{129}Xe by the spin precession method are presented. Section 5 contains suggestions of further experiments and conclusive remarks. Preliminary results of the experiments described in this work have been reported earlier [5–8].

2. Measurement of Unperturbed Angular Correlations

2.1. The angular correlation function

The time-integrated unperturbed angular correlation function $W(\theta)$ is given by [9]

$$W(\theta) = \sum_{k=0}^{k_{\max}} A_k P_k(\cos\theta), \qquad k \text{ even} \tag{2.1}$$

where θ is the angle between the directions of the emitted radiations and P_k are the Legendre polynomials. The angular correlation coefficients A_k depend on the mixing ratios of the multipolarities of the emitted gamma rays and the spins and parities of the levels involved. In most cases the A_k are negligibly small for $k > 4$, and if $A_4 = 0$ as can be assumed for all cascades considered in this work, it is sufficient to measure the anisotropy

$$A = \frac{W(\pi)}{W(\pi/2)} - 1 \tag{2.2}$$

which is related to the A_2 coefficient by

$$A_2 = \frac{2 \cdot A}{3 + A}. \tag{2.3}$$

The presence of isotropic extranuclear fields causes an attenuation of the angular correlation which is usually expressed by the attenuation factors G_k ($\leqslant 1$). Equation (2.3) then transforms into

$$G_2 A_2 = \frac{2 \cdot A}{3 + A}. \tag{2.4}$$

2.2. *Cascades in* ^{127}I

2.2.1. *Source preparation*

The decay scheme of ^{127}Xe is given in Figure 1. The ^{127}Xe activity was obtained by irradiation of an enriched xenon gas sample of 1 mg enclosed in a quartz ampoule. The enriched gas (20% ^{124}Xe, 10% ^{126}Xe, 22% ^{128}Xe, 46% ^{129}Xe) was procured at Monsanto Mound Laboratory, Miamisburg, USA. The sample was irradiated during four days at a neutron flux of 10^{13} cm^{-2} s^{-1} at the reactor SAPHIR of EIR, Würenlingen, Switzerland. When the ^{125}Xe activity, which was produced simultaneously, had decreased to less than 0.1% of the ^{127}Xe activity, the sample was processed.

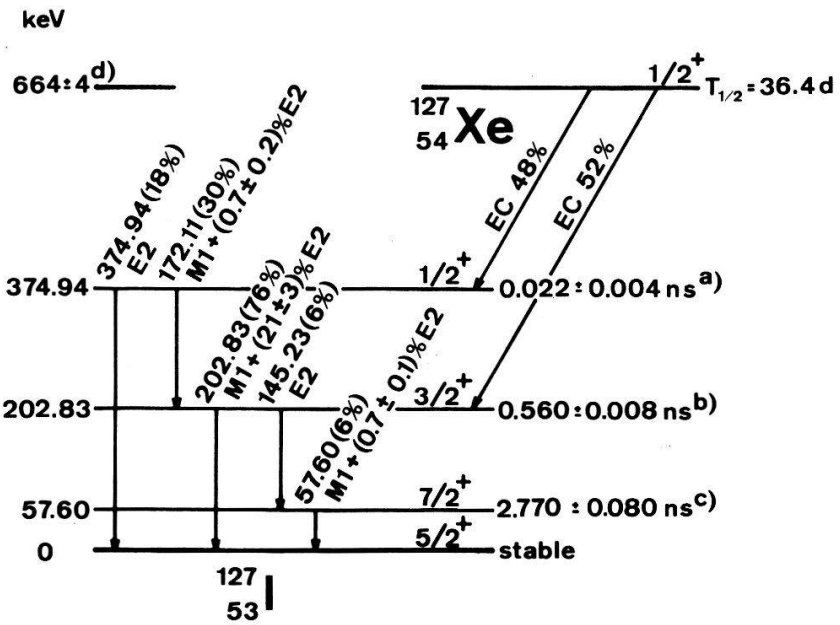

Figure 1
Decay scheme of ^{127}Xe, based on Ref. [10]. (a) Ref. [11]. (b) Refs. [12, 13]. (c) Refs. [14, 15, 16]. (d) Ref. [17].

The high gas density was produced by admixing inactive natural xenon gas (purity 99.99%) to the gas of the irradiated sample. Because depositing the xenon in the capsule in solid form did not yield the desired gas density, the gas had to be liquefied. The liquid xenon was obtained by cooling the gas to -77°C and compressing it to a pressure above the vapor pressure, which is 4 atm at this temperature. The apparatus used for the source preparation is shown schematically in Figure 2. The quartz ampoule (Q) containing the irradiated sample was inserted into the cracker (Cr), and the system was evacuated with all valves except valve V_1 open. Then the valves V_2 and V_3 were closed and the trap (T) was cooled with liquid nitrogen. Inactive xenon gas was admitted into the buffer volume (B) by opening valve V_1 and its amount was determined with the manometer M_1. Then valve V_1 was closed and the xenon was deposited in the trap by opening valve V_2. This procedure was repeated several times until a sufficient amount of xenon had been deposited in the trap. Then the valves V_2 and V_5 were closed and the sample ampoule was cracked. By cooling the steel capsule (Ca) with liquid nitrogen a considerable amount ($\simeq$40%) of the active gas was deposited in the capsule. Then valve V_4 was closed and the closing

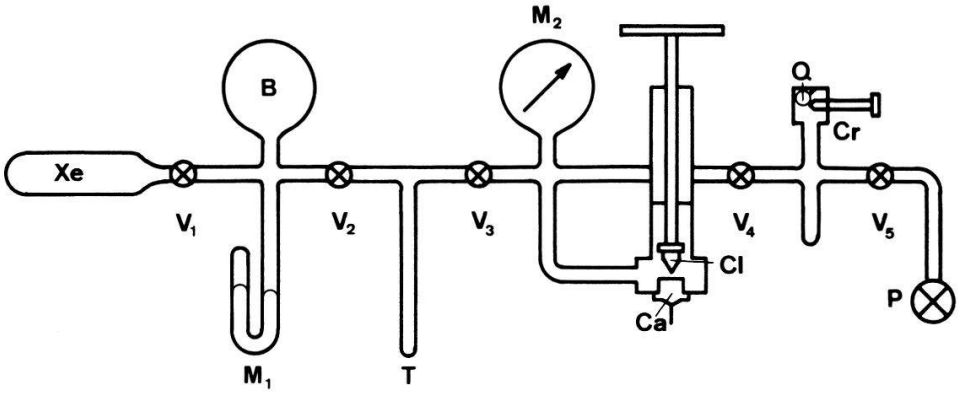

Figure 2
Filling apparatus (schematically). The symbols are explained in the text.

(Cl) was screwed a few turns onto the capsule. After opening valve V_3 the trap was warmed up, until the desired pressure ($\simeq 9$ atm) had built up, which was measured with the manometer M_2. Then valve V_3 was closed and the liquid nitrogen cooling the capsule was replaced by a mixture of dry ice and acetone. The capsule was reopened until an equilibrium had been reached, then the closing was screwed tightly onto the capsule. Because the inclinations of the cones of the capsule and the closing differed by about 1°, a cold welding occurred where the surfaces met and sealed the capsule. Details of the steel capsule and the closing are shown in Figure 3. The diameter of the cylindrical volume (V) was 1.1 mm, the wall was 0.2 mm thick. The xenon amount in the capsule was determined from the weight difference of capsule and closing full and empty. The gas density obtained was $\rho = 2.6 \pm 0.2\ \mathrm{g\,cm^{-3}}$.

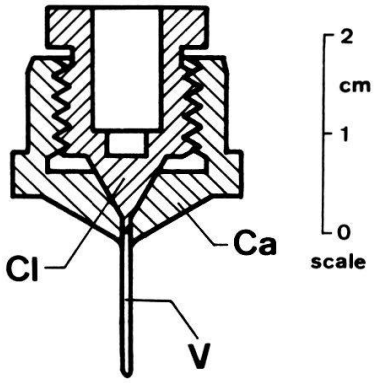

Figure 3
Steel capsule (Ca) and closing (Cl). The volume (V) contained the active gas.

2.2.2. Measurements and evaluation

The detector geometry and the electronic set-up are shown in Figures 4 and 5, respectively. For the measurement of the gamma spectra a Ge(Li) detector was employed. The adc was gated by pulses coming from a single-channel analyzer, whose window was centered at the desired energy in the spectrum of the movable NaI(T1) detector. The time resolution of the system was $2\tau = 30$ ns. The coincidences were recorded for a period of 10 min alternating the position between 90° and 180°. Before and after each coincidence measurement the delays of the fast pulses were detuned and chance coincidences were measured for a period of 2 min. The chance coincidence rate was up to 10% of the true rate. For the cascades 172–203 keV and 172–145 keV the single-channel was centered at 172 keV. A typical coincidence

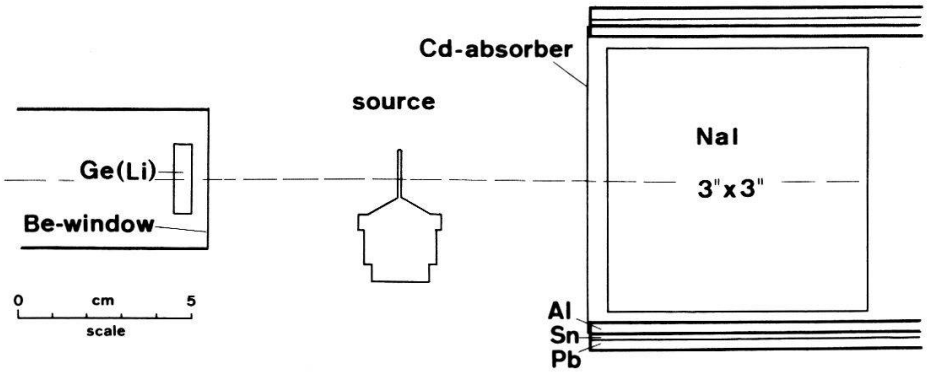

Figure 4
Detector geometry for the anisotropy measurements.

spectrum is given in Figure 6a. For the 145–58 keV cascade, the presence of scattered 172 keV gamma rays beneath the 58 keV peak required a modification of the measuring procedure. For this cascade the NaI(T1) spectrum was recorded gated by the pulses of the single-channel which was centered at 145 keV in the Ge(Li) spectrum. From the relative intensity of the weak 203 keV line in the coincidence spectrum the contribution of the scattered 172 keV quanta could be determined. A typical coincidence spectrum is given in Figure 6b (the solid line denotes the chance coincidence contribution).

All spectra were examined for peak shifts or recording errors, then they were summed. The coincidence rates determined by the areas beneath the peaks were

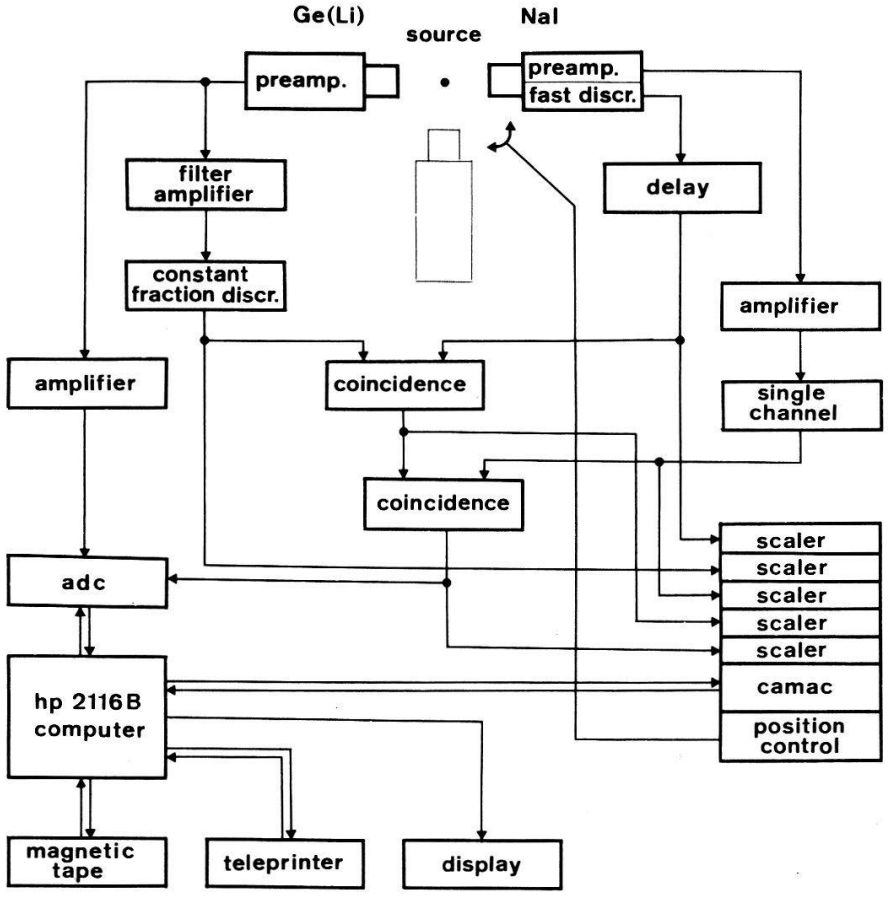

Figure 5
Electronic set-up (schematically)

calculated by fitting gaussians with a linear background to the spectrum and were normalized by the single-channel counting rates of the movable NaI(T1) detector. For the 145–58 keV cascade the normalization was performed using the single-channel counting rates of both detectors.

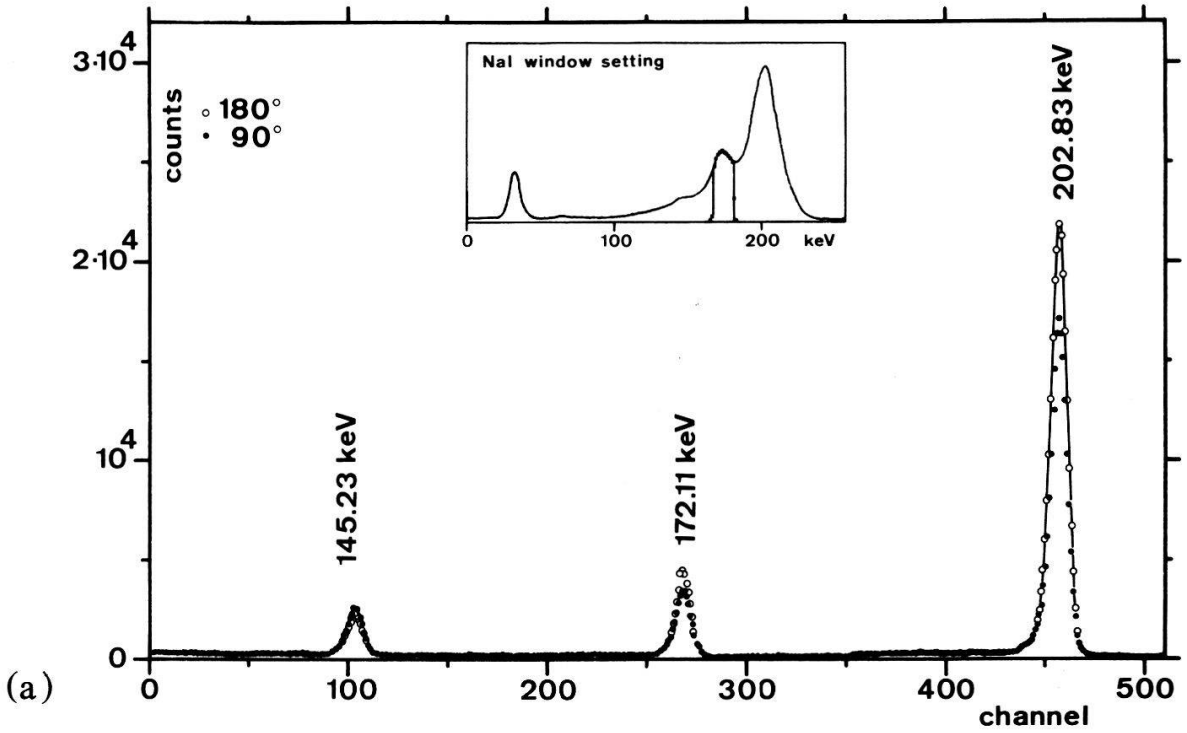

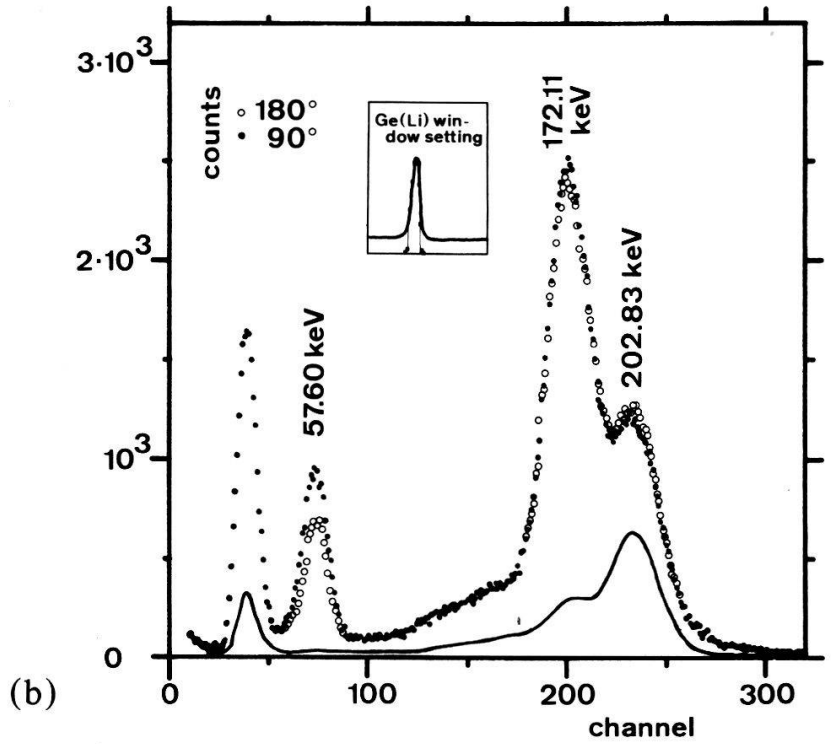

Figure 6
(a) Spectrum of ^{127}Xe, coincident with the 172 keV transition. (b) Spectrum of ^{127}Xe, coincident with the 145 keV transition.

2.2.3. Corrections

The corrections applied are summarized in Table I. The finite solid angle corrections were interpolated from tables by Camp [18] for the Ge(Li) detector and from tables by Yates [19] for the NaI(Tl) detector. The uncertainties of these corrections which arose mainly from the geometry were about 0.5% for both detectors. Since the detectors cannot distinguish between the full energy radiation and the forward Compton scattered gamma rays, if the energy loss does not exceed the line width, the effective solid angle is enlarged. The influence of this scattered radiation was estimated from a Monte Carlo calculation of the energy distribution. Since the effect is small, multiple processes were neglected. Scattering inside the source and in the walls were taken into account. The effect was found to be negligibly small for energies above 100 keV.

Table I
A_2 measurements

Isotope	^{127}I		
cascade	172–203 keV	172–145 keV	145–58 keV
		Correction factors on A_2	
[a])	0.842	0.842	0.827
[b])	0.984	0.983	0.983
[c])			0.956 ± 0.005
[d])			1.038 ± 0.003
		A_2	
[e])	0.2170 ± 0.0028	−0.052 ± 0.011	−0.2234 ± 0.0067
	0.2233 ± 0.0037[f])		−0.128 ± 0.032[f])
	0.216 ± 0.002[g])		−0.2254 ± 0.0050[h])
Mixing ratio	$\delta_{172} = 0.088 \pm 0.011$		

Isotope	^{125}I	^{129}Xe
cascade	55–188 keV	196–40 keV
	Correction factors on A_2	
[a])	0.845	0.846
[b])	0.981	0.981
[c])	0.955 ± 0.004	
[d])	0.981 ± 0.002	0.990 ± 0.002
	A_2	
[e])	0.229 ± 0.008	−0.159 ± 0.007
	0.235 ± 0.012[i])	−0.157 ± 0.016[k])
Mixing ratio	$\delta_{55} = 0.026 \pm 0.010$	

[a]) Finite solid angle correction NaI(Tl).
[b]) Finite solid angle correction Ge(Li).
[c]) Correction due to small angle Compton scattering in the source and the source container.
[d]) Correction due to self-absorption in the source and finite source dimensions.
[e]) Present work.
[f]) Ref. [21].
[g]) Ref. [4].
[h]) Calculated from Refs. [14, 21, 26].
[i]) Ref. [10].
[k]) Ref. [33].

The absorption inside the source required a further correction. For the low energy radiation the absorption is strong enough to cause an anisotropy even if the radiation is emitted isotropically. To calculate this correction a Monte Carlo program was employed. A point inside the source and the directions of the two gamma rays were chosen at random. The probability of registering a coincidence was calculated from the paths inside the source and the absorption coefficients assuming isotropic emission. For the 145–58 keV cascade a ratio $C(180°)/C(90°) = 0.967 \pm 0.003$ was obtained. The values given in Table I represent the effect on the A_2 coefficient. The correction for finite source dimensions is included in these values. For cascades with energies above 100 keV the self-absorption is negligible.

No corrections were necessary due to P_4 terms in the correlation. For the 172–203 keV cascade A_4 is zero, since the 203 keV level has spin 3/2 [20, 21], and for the 145–58 keV cascade A_4 is negligibly small because the 58 keV is a $M1$ transition with only a small $E2$ admixture [20].

2.2.4. Results and discussion

The K capture in ^{127}Xe and the following rearrangement of the atomic shell leave a strongly ionized atom within a time less than 10^{-14} s after the electron capture [31]. The effect of the hyperfine interaction of these strongly ionized atoms on the correlation can be observed in low-density gaseous sources (cf. Section 3). In a high-density gaseous source the vacancies in the electronic shell are refilled by collisions with neighboring atoms. The collision frequency is high in the beginning, when the atom has a high recoil velocity from the ν-emission and the ionization causes a collision cross-section larger than the geometric [4], and decreases to some 10^{12} s^{-1} for a density of about 2 g cm^{-3}, when thermal equilibrium is reached and the ionization has been reduced to minimum.

In this situation two mechanisms that can cause an attenuation of the angular correlation must be considered: First, the hyperfine interaction of the free atom which is isotropic and stationary during the free flight time of the atom, and second, time-dependent extranuclear fields which are induced by the deformation of the atom during the collisions. For the density of the source employed in the present experiment the duration of a collision $\Delta t \sim 10^{-12}$ s is comparable with the average time between two collisions $\tau_{\text{coll}} = 5 \cdot 10^{-13}$ s (calculated from thermal velocity and the radius of the I^- ion [22]). Therefore, the total interaction must be described by a combination of fluctuating electric and magnetic fields characterized by a correlation time τ_c which describes the combined effects of both mechanisms. Aspects of this situation have been treated in the literature [23–25]. In all cases the attenuation coefficient is given by a relation

$$G_2 = (1 + \lambda_2 \tau_n)^{-1} \tag{2.5}$$

if the following conditions are fulfilled:

(i) The fluctuation is fast ($\tau_c \ll \tau_n$), and

(ii) the precession frequency of the nuclear spin is small compared to τ_c^{-1} ($\sqrt{\lambda_2 \tau_c} \ll 1$).

The coefficient λ_2 describes the strength of the interaction and is proportional to the square of a suitable average of the interaction energy. Since the lifetimes τ_n in the cascades considered in this work are of the order 10^{-9} s and τ_c is of the order 10^{-12} s, the condition (i) is met in all cases. In order to show that the condition (ii) is fulfilled,

the interaction strength given by Gygax [4] is taken as an estimate. From this $\sqrt{\lambda_2 \tau_c} = 5 \cdot 10^{-3}$ is obtained. Therefore, the given form of the attenuation coefficient (2.5) describes the present situation.

For the 145–58 keV cascade all parameters determining the angular correlation coefficient A_2 are known from other experiments (Refs. [14, 21, 26]). The good agreement of the present result $A_2 = -0.2234 \pm 0.0067$ with the value calculated from these data $A_2 = -0.2254 \pm 0.0050$ shows that the correlation is unperturbed within 5% ($\lambda_2 \tau_n < 0.05$).

For the 172–203 keV cascade the angular correlation coefficient is not known. However, taking the ratio λ_2 (203 keV)/λ_2 (58 keV) $\simeq 2$ from Gygax [4] the estimate $\lambda_2 \tau_n < 0.02$ is obtained. Therefore, we conclude that the angular correlations of the 172 keV cascades are unperturbed in a high-density gaseous source. From the good agreement of the angular correlation coefficient of the 203 keV cascade measured with a metallic source [21] with the present result it can be concluded that the angular correlation in the metallic environment is also unperturbed for this cascade.

From internal conversion experiments [12] an upper limit for the mixing ratio of the 172 keV transition $|\delta_{172}| < 0.1$ and the mixing ratio of the 203 keV transition $\delta_{203} = 0.516 \pm 0.043$ are known[2]). Employing the latter, a mixing ratio $\delta_{172} = 0.088 \pm 0.011$ is deduced from the present measurement of the 172–203 keV cascade. From the 172–145 keV cascade the value $\delta_{172} = 0.076 \pm 0.045$ is obtained which is compatible.

The A_2 coefficient of the 172–58 keV correlation can be determined from the mixing ratios of the 172 keV and 58 keV transitions. The result $A_2 = 0.107 \pm 0.006$ is compatible with the value reported by Leisi [21] $A_2 = 0.15 \pm 0.07$, although the latter is probably attenuated due to perturbations.

2.3. The 55–188 keV cascade in ^{125}I

2.3.1. Source preparation and measurements

The decay scheme of ^{125}Xe is given in Figure 7. The ^{125}Xe activity was obtained by 8 hour irradiations of enriched xenon gas samples (see 2.2.1). The high density sources were prepared employing the procedure described above (2.2.1). The densities obtained ranged between 2.5 g cm^{-3} and 2.9 g cm^{-3}. The detector geometry and the electronic set-up were the same as for the ^{127}Xe measurements. A typical coincidence spectrum is shown in Figure 8. The small peak above the 55 keV line is due to a contamination of ^{127}Xe in the source (58 keV). Since the peaks are well separated, this contamination did not disturb the measurements. The corrections taken into account are listed in Table I along with the results.

2.3.2. Results and discussion

The 55–188 keV cascade in ^{125}I is very similar to the 172–203 keV cascade in ^{127}I. Apart from the identical spin sequence the lifetimes of the intermediate levels are equal within 10%. Furthermore, Gygax [4] obtained almost identical slopes of the attenuation factor G_2 as a function of the source pressure. This indicates, that the attenuations of the correlation of both cascades are not significantly different.

---

[2]) The sign of the mixing ratios is defined according to Biedenharn and Rose [27] throughout this work.

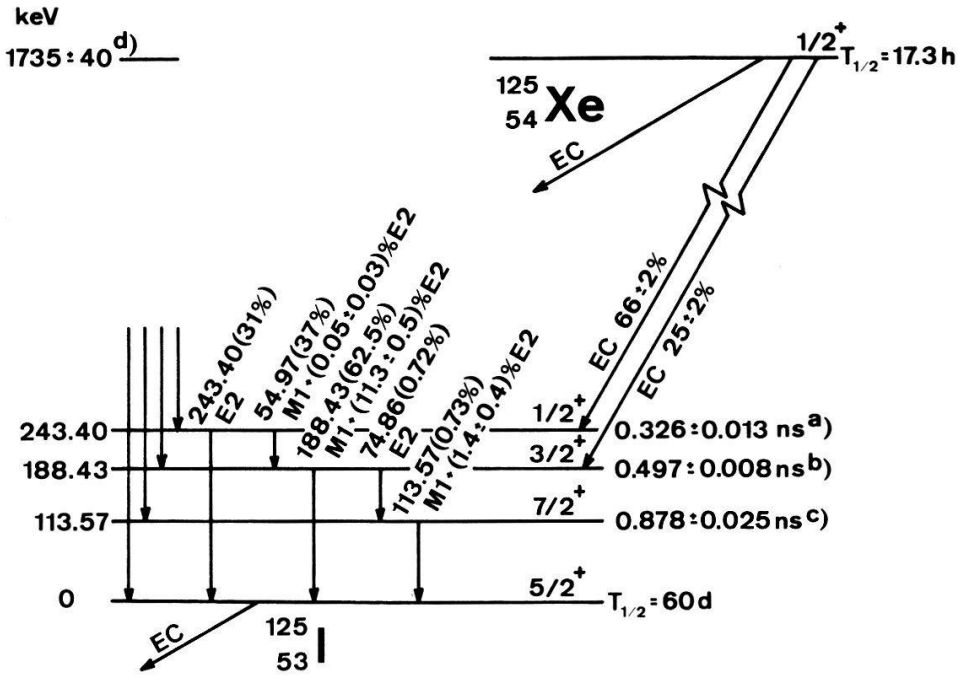

Figure 7
Decay scheme of ^{125}Xe, based on Ref. [10]. (a) Refs. [13, 28]. (b) Refs. [12, 13, 28]. (c) Refs. [13, 14]. (d) Ref. [29].

Accordingly, a negligible attenuation of the 55–188 keV cascade measured in a high-density gaseous environment can be assumed.

The mixing ratios given by Geiger [10] from electron conversion measurements are $\delta_{55} = \pm 0.022 \pm 0.009$ for the 55 keV transition and $\delta_{188} = 0.357 \pm 0.009$ for the 188 keV transition. Employing the latter value a mixing ratio $\delta_{55} = +0.026 \pm 0.010$

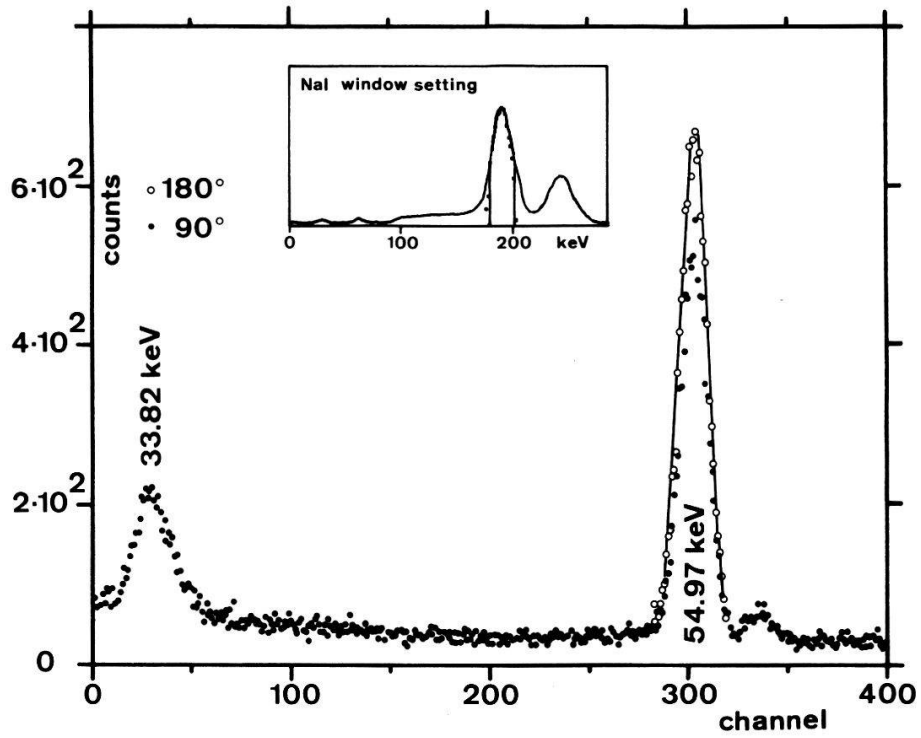

Figure 8
Spectrum of ^{125}Xe, coincident with the 188 keV transition (part of the statistics).

is obtained from the present experiment, the absolute value of which is compatible with Geiger's result. The angular correlation coefficient obtained with a metallic source [10] agrees well with the present result. From this it can be concluded that also the metallic environment does not perturb the correlation.

2.4. *The 196–40 keV cascade in* ^{129}Xe

2.4.1. *Source preparation and measurements*

The decay scheme of ^{129m}Xe is shown in Figure 9. The ^{129m}Xe activity was produced by the process $^{127}I(n, \gamma)^{128}I \rightarrow (25\ min) \rightarrow {}^{128}Xe(n, \gamma)^{129m}Xe$. Samples of

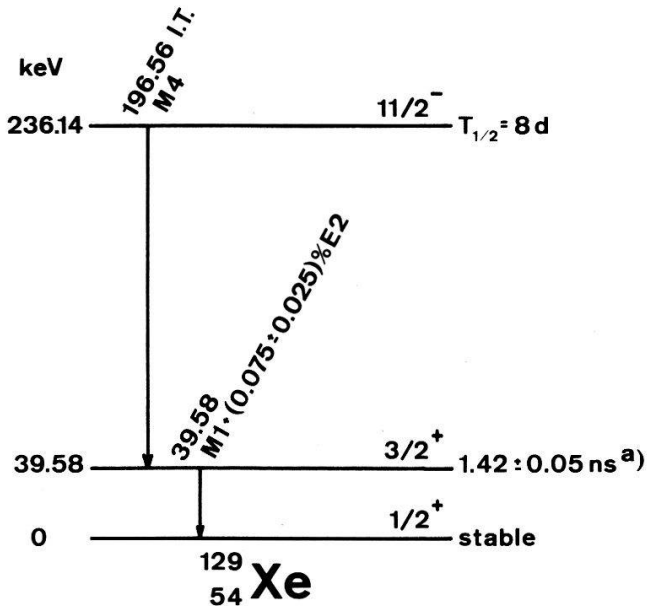

Figure 9
Decay scheme of ^{129m}Xe, based on Ref. [14].

10 mg KI enclosed in quartz ampoules were irradiated during three weeks at MOL, Belgium, at a neutron flux of $5 \cdot 10^{14}\ cm^{-2}\ s^{-1}$. From the irradiated samples the xenon was extracted and purified using the procedure described by Leisi [31], except for an improved pressure determination by use of Pirani manometers. The purified gas was transferred into spherical pyrex ampoules with 12 mm outer diameter and 1 mm thick walls. The two sources had pressures of 6 ± 1 and 8 ± 1 torr, respectively, and contained mainly ^{128}Xe (0.01% ^{129}Xe and 0.02% ^{129m}Xe at preparation time). The detector geometry and the electronic set-up were identical to those used in the ^{127}Xe measurements. A typical coincidence spectrum is given in Figure 10. The data evaluation proceeded as described above (2.2.2).

2.4.2. *Results and discussion*

Since the xenon atom has no hyperfine interaction in its ground state because xenon is a noble gas, and since the gamma ray emission leading to the intermediate level cannot alter the electronic state[3]), the angular correlation measured in a gaseous source is free from any perturbation, provided the gas pressure is so low that there are no collisions with neighboring atoms during the lifetime of the intermediate

[3]) The recoil energy after the emission of the 196 keV gamma (~0.2 eV) is smaller than the smallest excitation energy of the xenon atom.

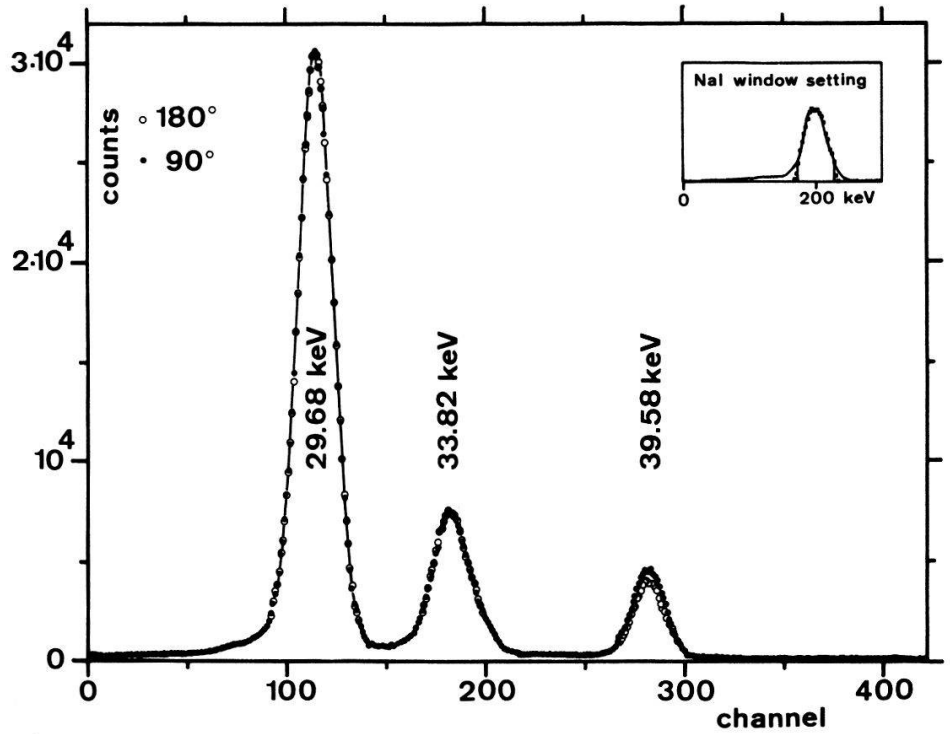

Figure 10
Spectrum of ^{129m}Xe, coincident with the 196 keV transition.

nuclear state. At a pressure of 10 torr the free flight time of the atom is $\tau_{coll} = 100$ ns (calculated from the recoil velocity after the 196 keV gamma emission), and hence the probability for a collision during the nuclear lifetime is $\tau_n/\tau_{coll} = 1.4\%$. Since the atom cannot be excited by a collision, only the influence of extranuclear fields during the collision must be considered. Even if these fields would reduce the correlation to the hard core value ($G_2 = 0.2$) for those atoms that suffer a collision during the nuclear lifetime, the total attenuation would be weak ($G_2 = 0.99$). However, since very strong fields are required to realize the hard core attenuation, an even weaker and therefore negligible attenuation is to be expected in the present case.

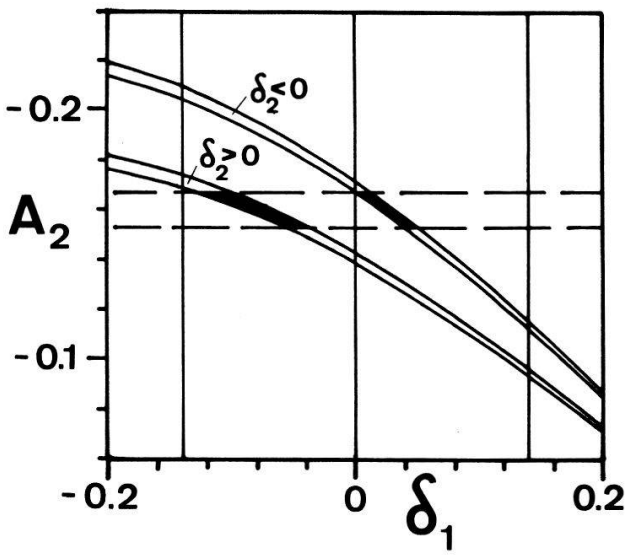

Figure 11
Angular correlation coefficient of the 196–40 keV cascade in ^{129}Xe versus mixing ratio of the 196 keV transition.

The correlation coefficient measured in the present experiment, $A_2 = -0.159 \pm 0.007$, is more precise than and in agreement with the value reported by Gygax [32], $A_2 = -0.157 \pm 0.016$. Geiger [14] gives a mixing ratio of $\delta_2^2 = (7.5 \pm 2.5) \cdot 10^{-4}$ for the 40 keV transition from electron conversion measurements. Based on this value a plot of the angular correlation coefficient as a function of the mixing ratio of the 196 keV transition δ_1 is given in Figure 11 showing that a positive sign of δ_2 implies an $E5$ admixture, while a pure $M4$ is only compatible with a negative δ_2. Thus the present measurement is compatible with the result of the electron conversion experiments that the $E5$ admixture is small and restricts the possible values of δ_1 to (95% confidence level):

$$-0.135 \leqslant \delta_1 \leqslant -0.028 \qquad \delta_2 > 0$$

$$-0.012 \leqslant \delta_1 \leqslant 0.069 \qquad \delta_2 < 0.$$

This restriction improves the upper limit $|\delta_1| \leqslant 0.14$ given by Geiger [33] from electron conversion experiments.

3. Resonance Measurements

3.1. The angular correlation function

The effect of a weak external magnetic field on the time-integrated angular correlation perturbed by a strong time-independent hyperfine interaction has been investigated by Leisi [1, 31, 34], according to whom the angular correlation of a cascade with $A_4 = 0$ observed in a plane perpendicular to the magnetic field B is given by:

$$W(\Phi) = D_0 + \sum_F D_{F2} \frac{\cos(2\Phi) - 2\gamma_F X \sin(2\Phi)}{1 + 4\gamma_F X^2} \tag{3.1}$$

where

$$X = g_J \mu_B B \tau_n / \hbar \tag{3.2}$$

and

$$\gamma_F = g_F/g_J = \frac{F(F+1) + J(J+1) - I(I+1)}{2F(F+1)}. \tag{3.3}$$

Φ is the angle between the emission directions of the gamma rays, I and τ_n are the spin and the lifetime of the intermediate nuclear state, g_J and g_F are the splitting factors associated with the electronic state J and the states of total angular momentum F and μ_B is the Bohr magneton. The coefficients D_0 and D_{F2} are given by:

$$D_0 = 1 + \tfrac{1}{4} A_2 G_2 \tag{3.4}$$

and

$$D_{F2} = \frac{3}{4} A_2 \frac{(2F+1)^2}{2J+1} \begin{Bmatrix} F & F & 2 \\ I & I & J \end{Bmatrix}^2. \tag{3.5}$$

G_2 denotes here the hard-core attenuation coefficient of the same angular correlation in absence of a magnetic field. The derivation of the formulas (3.1)–(3.5) is based on

the assumption that the hyperfine interaction is strong enough, i.e. that the splitting is large compared with the natural width of the nuclear level:

$$|E_F - E_{F'}| \gg \hbar/\tau_n. \tag{3.6}$$

For special angles Φ the following expressions are obtained:

$$W(\pi) - W(\pi/2) = 2\sum_F \frac{D_{F2}}{1 + 4\gamma_F^2 X^2} \tag{3.7}$$

$$W(3\pi/4) - W(5\pi/4) = -2\sum_F \frac{2D_{F2}\gamma_F X}{1 + 4\gamma_F^2 X^2}. \tag{3.8}$$

Thus a measurement of the angular correlation at these angles will show a particularly simple resonance behavior.

3.2. *Choice of source pressure and source preparation*

The condition (3.6) is well satisfied for nuclear lifetimes of the order of 10^{-9} s [1, 31] in cascades following electron capture, which leads because of the subsequent rearrangement of the electronic shell to highly charged ions. From this ionization a strong hyperfine interaction results, unless $J = 0$ or the electronic shell is refilled during the nuclear decay. In a gas, additional electrons may come only from collisions with neutral atoms. At low pressures of a few torr, however, the mean free flight time of the atom can be enlarged to values substantially exceeding the nuclear lifetime.

The activity was produced by irradiation of separated isotopes of ^{124}Xe and ^{126}Xe absorbed in Al-foil. The foils were obtained from the Atomic Energy Research Establishment, Harwell, England. The active xenon was extracted after the irradiation by melting the foil and was processed as described for the ^{129}Xe sources (2.4.1). The source pressures obtained are listed in Table II.

Table II
Results from resonance measurements

Isotope cascade	^{125}I 55–188 keV		^{127}I 172–203 keV
	Present work		Ref. 1
p (torr)	2 ± 1	$< .1$	2 ± 1
ΔB_1 (Gauss)	400 ± 160	237 ± 46	195 ± 41
A_0	0.040 ± 0.007	0.053 ± 0.006	0.045 ± 0.004
A_∞	0.049 ± 0.009	0.054 ± 0.009	
p (torr)	3.6 ± 1.4	<1	
ΔB_2 (Gauss)	234 ± 69	204 ± 52	
B_0	0.029 ± 0.005	0.034 ± 0.006	
B_∞	0.003 ± 0.001	-0.003 ± 0.001	

3.3. *Measurements and evaluation*

The angular correlation was measured as a function of the external magnetic field which was applied perpendicular to the detector plane. The electronic set-up

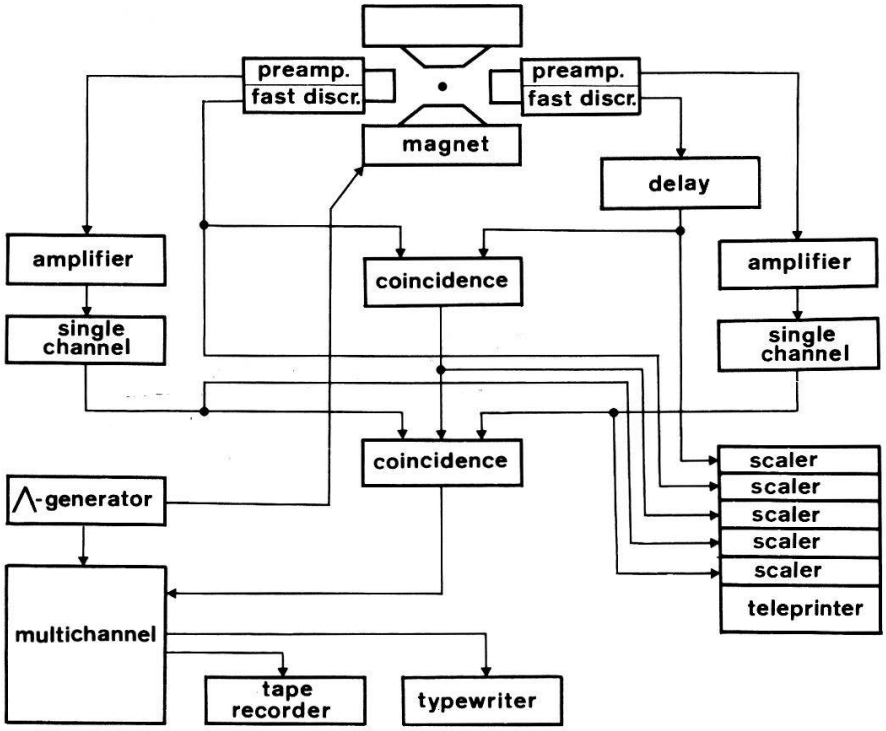

Figure 12
Electronic set-up used for the resonance measurements.

used for the measurements is shown in Figure 12. A 3″ × 3″ NaI(T1) detector with a special magnetic shielding and a 2″ × 2″ NaI(T1) detector with a light pipe were used. The effect of the magnetic field on the detectors was determined and found to be negligible. The desired energy ranges were selected by single-channel analyzers for both detectors. The coincidences were stored in a multichannel analyzer, in which the channel number was determined by the output of a Bell 640 Gaussmeter measuring the magnetic field. The field was swept continuously by a triangular signal of 0.02 s^{-1} between 0 and 2 kGauss for both field directions. The coincidences were recorded at 90° and 180° or at 135° and 225°, respectively, along with chance coincidences.

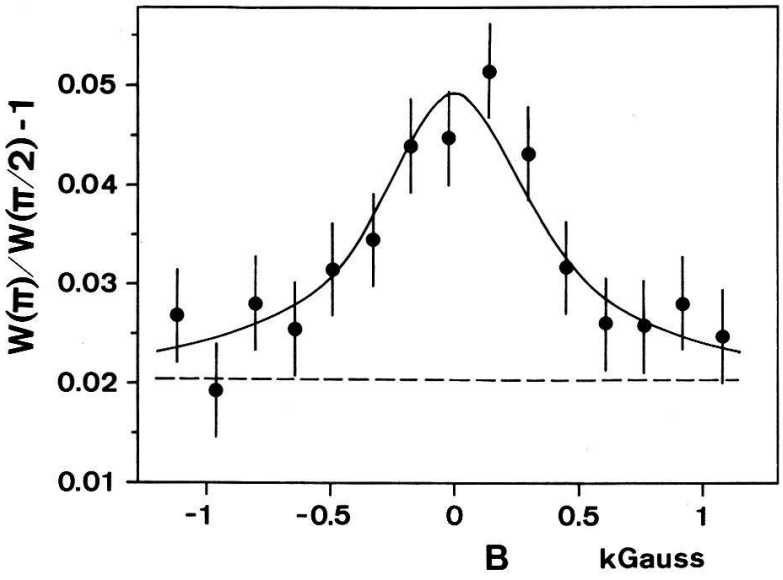

Figure 13
Anisotropy as a function of the magnetic field for the 55–188 keV cascade in ^{125}I.

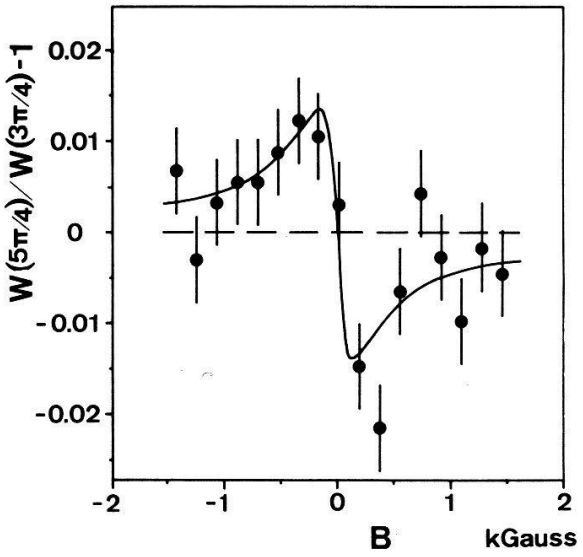

Figure 14
$W(5\pi/4)/W(3\pi/4) - 1$ as a function of the magnetic field for the 55–188 keV cascade in ^{125}I.

The coincidence rates were normalized by the single channel counting rates of the movable detector, and the averages over channel subgroups were calculated. The resulting relative count differences are shown in Figures 13 to 16. The solid lines represent a fit of

$$A_0\left\{1 + \left(\frac{B}{\Delta B_1}\right)^2\right\}^{-1} + A_\infty \tag{3.9}$$

or

$$B_0 \frac{B}{\Delta B_2}\left\{1 + \left(\frac{B}{\Delta B_2}\right)^2\right\}^{-1} + B_\infty \tag{3.10}$$

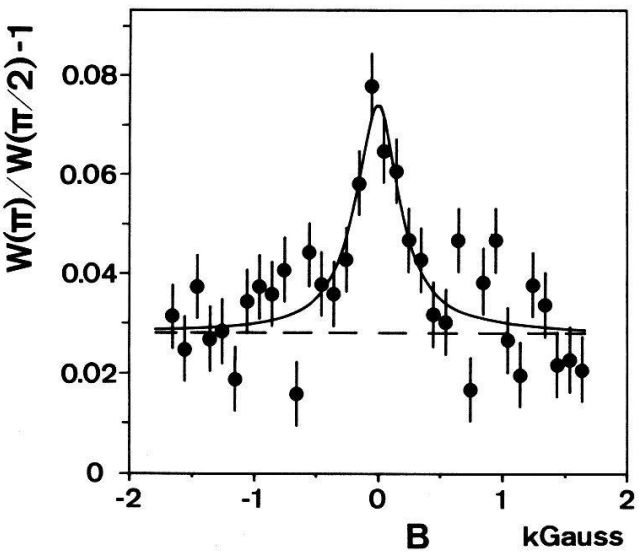

Figure 15
Anisotropy as a function of the magnetic field for the 172–203 keV cascade in ^{127}I.

for the measurements at 90°/180° or at 135°/225°, respectively. The fit parameters A_0, A_∞, ΔB_1 and B_0, B_∞, ΔB_2 denoting the amplitudes of the resonance, the constant background and the resonance width, respectively, are listed in Table II.

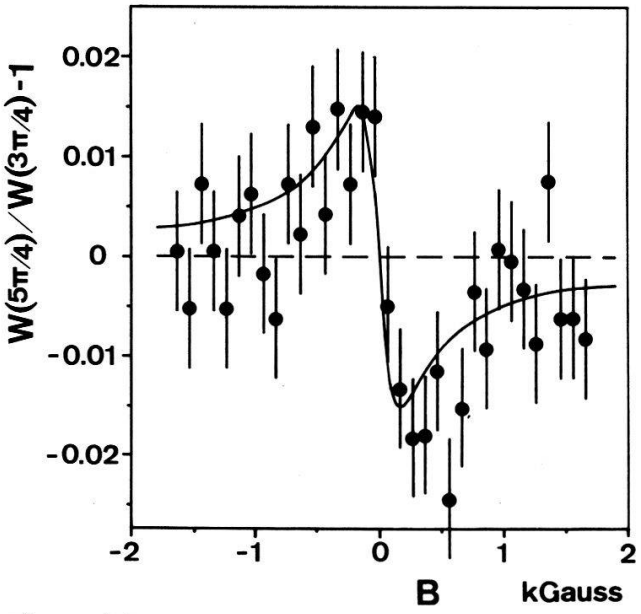

Figure 16
$W(5\pi/4)/W(3\pi/4) - 1$ as a function of the magnetic field for the 172–203 keV cascade in ^{127}I.

3.4. *Results and discussion*

The difference between A_∞ and B_∞ can be explained by a fraction of decays which do not show a resonance, e.g. electronic states with $J = 0$. These decays contribute only to the 90°/180° measurements and hence B_∞ is very small. Since the amplitude B_0 is only slightly smaller than A_0, only few terms in the sum (3.8) can be negative. This indicates that the majority of the contributing states has a positive splitting factor. The widths ΔB_1 and ΔB_2 are equal within experimental error. If the hyperfine interaction is strictly stationary, this width can be expressed as

$$\Delta B = \frac{\hbar}{2\mu_B \tau_n \langle|\gamma_F g_J|\rangle} \tag{3.11}$$

where $\langle|\gamma_F g_J|\rangle$ denotes a suitable average over different F states of a particular electronic state J and over the contributing electronic states. If the experiment is performed on a single atomic state, J and g_J are known and the expression $\langle|\gamma_F g_J|\rangle$ can be evaluated. Then the lifetime τ_n can be determined from a measurement of ΔB according to equation (3.11).

In the present experiment, however, two complications arise. First, the system consists of a set of many atomic states produced by the K capture. The parameters evaluated by the fit represent therefore average values. Second, the non-zero value of A_∞ indicates that the hyperfine interaction is not fully stationary [31], which would in principle increase the resonance width above the value given by (3.11). However, since very special conditions on atomic lifetimes would have to be realized in order to change ΔB appreciably, we conjecture that this effect is small. Therefore the value

$$\langle|\gamma_F g_J|\rangle = 0.45 \pm 0.05$$

deduced from the ΔB values of Table II and the known lifetimes (see Table III) is presumably representative for other K capture decays also. Since the hyperfine interaction after the K capture is extremely strong, the resonance condition (3.6) may

still be realized for very short lifetimes, particularly for heavy nuclei. Thus resonance experiments may possibly be used to measure short nuclear lifetimes.

4. Measurements of Magnetic Moments

4.1. The angular correlation function

The time-dependent angular correlation function in the presence of a vertical magnetic field B may be written as follows:

$$W(\theta, B, t) = \sum_{k=0}^{k_{\max}} A_k P_k(\cos\{\theta - \omega_B t\}) \tag{4.1}$$

where θ is the angle between the directions of the emitted radiations in the plane perpendicular to the magnetic field and $\omega_B = g\mu_N B/\hbar$ is the Larmor frequency with g denoting the gyromagnetic ratio and μ_N the nuclear magneton. From this expression the time-integrated correlation function can be calculated. The result for $k_{\max} = 2$ is:

$$W(\theta, B) = \left(A_0 + \frac{1}{4} A_2\right)\left\{1 + \frac{3A_2}{4 + A_2} \frac{\cos(2\theta - \operatorname{arctg} 2\omega_B \tau_n)}{\sqrt{1 + 4\omega_B^2 \tau_n^2}}\right\} \tag{4.2}$$

where τ_n is the nuclear lifetime. The precession angle $\omega_B \tau_n$ may be calculated easily from measurements of W at opposite magnetic fields ($B\uparrow$ and $B\downarrow$) and three angles: $\theta_0 = 3\pi/4$, $\theta_1 = \theta_0 + \phi$ and $\theta_2 = \theta_0 - \phi$. For an arbitrary angle ϕ the following expression is valid:

$$\omega_B \tau_n = \sin 2\phi \frac{W(\theta_0, B\downarrow) - W(\theta_0, B\uparrow)}{W(\theta_1, B\uparrow) + W(\theta_1, B\downarrow) - W(\theta_2, B\uparrow) - W(\theta_2, B\downarrow)}. \tag{4.3}$$

Obviously, the maximum effect is gained for $\phi = \pi/4$. Furthermore the expression is independent of solid angle corrections. From the precession angle the nuclear g-factor can be calculated if the lifetime of the level is known.

4.2. Measurements

The source preparation and the electronic set-up were the same as for the anisotropy measurements described in Section 2. For the shielding of the detectors against the strong magnetic field special care had to be taken. The 2″ × 2″ NaI(Tl) detector was equipped with a light pipe to allow the photomultiplier to be situated outside the area of strong field. The photomultiplier was shielded against the remaining field by μ-metal foil. For the Ge(Li) detector a shielding of pure iron was constructed. The effect of the magnetic field on the Ge(Li) was determined to be less than 0.06% on the counting rate and less than 0.03% on the peak center. For the NaI(Tl) detector these limits were 0.05% and 0.01%, respectively. The geometry of the detectors and the shielding is shown in Figure 17. The ^{125}Xe and ^{127}Xe sources had to be put slightly outside the detector plane, however, the evaluation according to equation (4.3) is not affected by this.

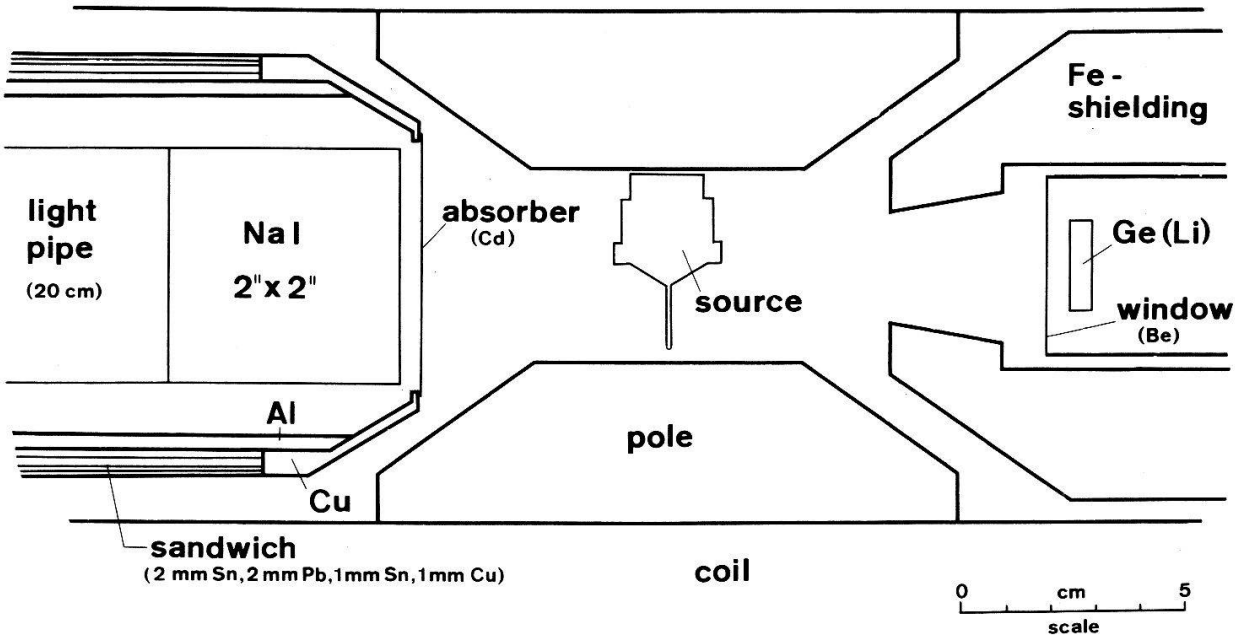

Figure 17
Geometry of the detectors, the magnet and the iron shielding used in the magnetic moment measurements.

A typical run started with recording the coincidences for both field directions at the angles $\pi/2$ and π. Then a series of measurements at the angle $3\pi/4$ was carried out changing the field direction after each period. The run was ended with measurements at the angles π and $\pi/2$ again for both field directions. Each measurement was preceded and followed by recording chance coincidences. Between two runs the electronic system was checked for shifts and a measurement of the anisotropy at zero field with identical geometry was carried out in order to determine a possible attenuation of the correlation by the magnetic field. From the anisotropy ratios $A(B)/A(0)$ which are given in Table III it can be concluded that the effects of the magnetic fields on the correlation are small.

The evaluation of the data proceeded as described for the anisotropy measurements (2.2.2). The resulting precession angles, the magnetic fields applied in the experiments and the nuclear moments are listed in Table III along with the level lifetimes on which the nuclear moments are based. The errors of the nuclear moments given in Table III arise mainly from the statistical errors. The effects of the magnetic field on the detectors are negligibly small compared to the statistical errors.

For the ^{125}I and the ^{127}I moments the effective magnetic field at the nucleus B_{eff} may be larger than the applied external field B_0 due to the so-called paramagnetic amplification. Since the correlation time τ_c is small compared to the nuclear lifetime and since the high collision frequency ensures that the thermal equilibrium is reached in a short time compared with the nuclear lifetime, the theory of Guenther and Lindgren [36] is applicable. Most likely, after the deionization the atom is in a state of I^+ [4]. We estimate the ratio B_{eff}/B_0 according to Guenther and Lindgren employing the magnetic hfs constant and the electronic splitting factor given by Martin and Corliss [37] for the I^+ ground state. The result $B_{\text{eff}}/B_0 = 1.02$ indicates a small

Table III
Nuclear moments of $3/2^+$ states

Isotope	^{125}I	^{127}I	^{129}Xe
Level (keV)	188	203	40
$A(B)/A(0)$	0.97 ± 0.05	0.98 ± 0.03	0.99 ± 0.01
Precession angle (radian)	0.048 ± 0.015	0.026 ± 0.004	0.074 ± 0.020
Lifetime (ns)	0.497 ± 0.008[a])	0.560 ± 0.008[b])	1.42 ± 0.05[c])
Field (kGauss)	13.8 ± 0.2	13.8 ± 0.2	21.7 ± 0.3
	Magnetic moments (nuclear magnetons)		
Present work	2.2 ± 0.7	1.05 ± 0.17	0.74 ± 0.20
Other authors		0.96 ± 0.07[d])	0.68 ± 0.30[e])
Theory[f])	1.00	1.13	0.57

[a]) Weighted average of Refs. [12, 13, 28].
[b]) Weighted average of Refs. [12, 13].
[c]) Weighted average of Refs. [14, 30].
[d]) Ref. [15] corrected for the different lifetime.
[e]) Ref. [38].
[f]) Calculated on the basis of Ref. [40].

effect on the anisotropy which is compatible with the measured anisotropy ratios $A(B)/A(0)$. The paramagnetic correction can thus be neglected in the present experiments.

4.3. Results and discussion

The magnetic moment of the 40 keV in ^{129}Xe, $\mu = 0.74 \pm 0.20$ nm, resulting from the present experiment is in agreement with the value given by Campbell [38], $\mu = 0.68 \pm 0.30$ nm. It is close to the magnetic moment of the ground state of ^{131}Xe $\mu = 0.691$ nm [39], which is also a $3/2^+$ neutron state. The theoretical value according to Kisslinger and Sorensen [40] is compatible with the present result.

The magnetic moment of the 203 keV state in ^{127}I measured in the present experiment, $\mu = 1.05 \pm 0.17$ nm, is in agreement with the theoretical value which we have calculated from the theory of Kisslinger [40] using the wavefunctions given by Langhoff [41]. It appears that the main contribution to the calculated value arises from one-phonon admixtures (the two-phonon contribution has been neglected). Svensson [15] reports a magnetic moment $\mu = 0.96 \pm 0.07$ nm (this value has been recalculated using the lifetime in Table III), which is compatible with the present result. Doubts about the presence of attenuations in the measurements of Svensson can be eliminated from the results of Section 2.2.4.

For the 188 keV level in ^{125}I the calculation of the theoretical value of the magnetic moment is somewhat difficult, because Kisslinger gives no wavefunctions for the $3/2^+$ level of this isotope. However, from the general behavior of the other states as well as from the similarity of both level schemes it can be concluded that the ^{125}I wavefunctions should not differ much from those of ^{127}I. Employing the wavefunctions of ^{127}I the value $\mu = 1.00$ is obtained for the magnetic moment of the 188 keV level in ^{125}I, which is of course close to the ^{127}I moment. However, the experiment is not quite in agreement with this result. The difference (almost two standard deviations) can hardly be explained by the choice of the wavefunctions, since even a radical

change would not yield agreement with the experimental result. It may be due to the neglection of two-phonon admixtures, although these corrections are generally small in the odd-mass iodine isotopes.

5. Conclusion

The present work shows that gaseous systems provide an interesting environment for performing various types of angular correlation experiments. Unperturbed angular correlations can be measured either at low pressure, if the atomic state has spin $J = 0$, or at high pressure, if the atom or ion is in a paramagnetic state. Apart from mixing ratios of nuclear transitions, magnetic moments of excited states can be measured in these systems. The possibility of varying easily and continuously the pressure of the gas allows one to choose the time-dependence of the perturbation and to explore the full range of relaxation phenomena. Measurements at low pressure on paramagnetic ions have shown that the resonance due to crossing Zeeman levels does behave as expected theoretically.

Further research in this field could be done by studying the angular correlation as a function of both the pressure and an externally applied magnetic field. It could be possible in this way to identify the electronic states which would allow one to determine e.g. quadrupole moments from the observed hyperfine splittings.

Acknowledgments

The author would like to thank Prof. Dr. J. P. Blaser for the opportunity to perform this work and Prof. Dr. H. J. Leisi for his constant interest and encouraging support. The assistance of F. N. Gygax, H. Dirren, F. C. Röhmer, D. Taqqu and R. Eichler is greatly appreciated. Thanks are due to G. H. Eaton for carefully reading the manuscript.

REFERENCES

[1] H. J. Leisi, Phys. Rev. *A1*, 1654 (1970).
[2] H. J. Leisi, Phys. Lett. *17*, 308 (1965).
[3] F. N. Gygax, J. Egger and H. J. Leisi, *Hyperfine Structure and Nuclear Radiations*, edited by E. Matthias and D. A. Shirley (North Holland, Amsterdam 1968), p. 948.
[4] F. N. Gygax, Thesis, Swiss Federal Institute of Technology, Zurich, 1971 (unpublished).
[5] Th. v. Ledebur, F. N. Gygax and H. J. Leisi, Helv. Phys. Acta *42*, 581 (1969).
[6] H. J. Leisi, Th. v. Ledebur and F. N. Gygax, *Angular Correlations in Nuclear Disintegration*, edited by H. van Krugten and B. van Nooijen (Rotterdam University Press, 1971), p. 444.
[7] Th. v. Ledebur and R. Eichler, Helv. Phys. Acta *46*, 50 (1973).
[8] Th. v. Ledebur, *Proceedings of the International Conference on Nuclear Physics*, Vol. I, edited by J. de Boer and M. J. Mang (North Holland, Amsterdam 1973), p. 257.
[9] H. Frauenfelder and R. M. Steffen, *Alpha-, Beta- and Gamma-Ray Spectroscopy*, edited by K. Siegbahn (North Holland, Amsterdam 1965), chapter XIX A.
[10] J. S. Geiger, Phys. Rev. *158*, 1094 (1967).
[11] H. Langhoff and D. Gföller, Nucl. Phys. *A127*, 379 (1969).
[12] J. S. Geiger and R. L. Graham, Nucl. Phys. *89*, 81 (1966).
[13] J. Kownacki, J. Ludzijewski and M. Moszynski, Nucl. Phys. *A107*, 476 (1968).
[14] J. S. Geiger, R. L. Graham, I. Bergström and F. Brown, Nucl. Phys. *68*, 352 (1965).
[15] A. G. Svensson, R. W. Sommerfeldt, L. O. Norlin and P. N. Tandon, Nucl. Phys. *A95*, 653 (1967).
[16] P. Thieberger, Ark. Fys. *22*, 127 (1962).

[17] W. D. SCHMIDT-OTT, W. WEIRAUCH, F. SMEND, H. LANGHOFF and D. GFÖLLER, Z. Phys. *217*, 282 (1968).
[18] D. C. CAMP and A. L. VAN LEHN, Nucl. Instr. Meth. *76*, 192 (1969) and Nucl. Instr. Meth. *87*, 147 (1970).
[19] M. J. L. YATES, *Alpha-, Beta- and Gamma-Ray Spectroscopy*, edited by K. SIEGBAHN (North Holland, Amsterdam 1965), appendix 9.
[20] J. S. GEIGER, Phys. Lett. *7*, 48 (1963).
[21] H. J. LEISI, Nucl. Phys. *76*, 308 (1966).
[22] LANDOLT-BÖRNSTEIN, *Zahlenwerte und Funktionen*, 6. Auflage (Springer, Berlin).
[23] A. Abragam and R. V. Pound, Phys. Rev. *92*, 943 (1953).
[24] C. SCHERER, Nucl. Phys. *A157*, 81 (1970).
[25] M. BLUME, Nucl. Phys. *A167*, 81 (1971).
[26] P. N. TANDON, S. H. DEVARE and H. G. DEVARE, *Congrès International du Physique Nucleaire, Paris 1964*, Vol. II, p. 56.
[27] L. C. BIEDENHARN and M. E. ROSE, Rev. Mod. Phys. *25*, 729 (1953).
[28] Y. S. HOROWITZ, R. B. MOORE and R. BARTON, Can. J. Phys. *45*, 101 (1967).
[29] J. LUDZIJEWSKI, W. KLAMRA and J. KOWNACKI, Acta Phys. Pol. *B1*, 189 (1970).
[30] O. C. KISTNER, S. MONARO and A. SCHWARZSCHILD, Phys. Rev. *137*, B23 (1965).
[31] H. J. LEISI, Phys. Rev. *A1*, 1662 (1970).
[32] F. N. GYGAX, R. F. JENEFSKY and H. J. LEISI, Phys. Lett. *B32*, 359 (1970).
[33] J. S. GEIGER, R. L. GRAHAM and F. BROWN, Can. J. Phys. *40*, 1258 (1962).
[34] H. J. LEISI, Ann. Phys. *84*, 39 (1974).
[35] K. ALDER and R. M. STEFFEN, Ann. Rev. Nucl. Sci. *14*, 429 (1964).
[36] C. GUENTHER and I. LINDGREN, *Perturbed Angular Correlation*, edited by E. KARLSSON, E. MATTHIAS and K. SIEGBAHN (North Holland, Amsterdam 1964), p. 357.
[37] W. C. MARTIN and C. H. CORLISS, J. Research *A64*, 443 (1960).
[38] L. E. CAMPBELL, G. J. PERLOW and N. C. SANDSTRÖM, *Hyperfine Structure and Nuclear Radiations*, edited by E. MATTHIAS and D. A. SHIRLEY (North Holland, Amsterdam 1968), p. 161.
[39] D. BRINKMANN, Helv. Phys. Acta *41*, 367 (1968).
[40] L. S. KISSLINGER and R. A. SORENSEN, Rev. Mod. Phys. *35*, 853 (1963).
[41] H. LANGHOFF, Nucl. Phys. *63*, 425 (1965).